Schottky-barrier electroreflectance of Ge: Nondegenerate and orbitally degenerate critical points

D. E. Aspnes
Bell Laboratories, Murray Hill, New Jersey 07974
(Received 19 May 1975)

Critical-point energies, broadening parameters, line-shape asymmetries, interband reduced masses, and polarization anisotropies are measured for the E_0, $E_0+\Delta_0$, E_1, $E_1+\Delta_1$, E_0', $E_0'+\Delta_0'$, $E_0'+\Delta_0'+\Delta_0$, E_2, E_1', $E_1+\Delta$, and $E_1'+\Delta_1'+\Delta_1''$ transitions in Ge using the Schottky-barrier electroreflectance (ER) method. The Keldysh-Konstantinov-Perel' (KKP) approximation for orbitally degenerate critical points is adapted to heavy holes and to Franz-Keldysh oscillations. Stark-shift effects are shown to be important only for energies within $4(\hbar\Omega)^3/E_g^2$ of E_g, negligible in this experiment. The KKP prediction that orbitally degenerate ER line shapes are represented as a linear superposition of nondegenerate line shapes is verified by separating explicitly the light-hole and heavy-hole contributions to the E_0 structure at intermediate fields. The polarization anisotropies are in qualitative agreement with KKP predictions, but the light-hole spectrum is much too large. Therefore, either the KKP matrix-element magnitudes or the calculated densities of states do not represent correctly the experimental conditions. Low-field line-shape asymmetries for E_0 and $E_0+\Delta_0$ are in excellent agreement with two-dimensional model density-of-states calculations. We observe a cusp less than 2 meV wide at threshold on spectra for which the intrinsic energy scale $\Omega\simeq 40$ meV, verifying remarkably well the prediction of a functional singularity at threshold in ER theory. The E_1 and $E_1+\Delta_1$ line shapes show polarization anisotropies of 1.32 ± 0.02 and 1.20 ± 0.02 at 300 and 10 K, respectively, for [110] fields, compared to a theoretical value of 4/3. Significant field-dependent polarization anisotropies are observed for the E_0' triplet, in qualitative agreement with the KKP approximation and in contrast to the predictions of nondegenerate theory. Heavy-electron–hole transitions appear to dominate the center structure of the E_0' triplet. The polarization anisotropy of 1.85 observed for the E_2 transition shows that the critical point responsible is a saddle point. The E_1' structures are resolved into three components. The larger energy separation, 266 ± 10 meV, for the two lower components of points responsible is not the same as that for the E_1 transitions, which have a spin-orbit splitting of 184 ± 2 meV.

I. INTRODUCTION AND CONCLUSIONS

The Schottky-barrier electroreflectance technique[1,2] is well suited to the spectroscopy of semiconductors.[3] At low fields, the third-derivative nature[4-6] of low-field electroreflectance (ER) spectra permits critical-point structures closely spaced in energy to be resolved. Low-field ER spectra that are determined entirely by the intrinsic properties of the material are easy to obtain in the Schottky-barrier configuration, because these spectra simply scale linearly in the modulating potential.[5,6] At intermediate fields, Franz-Keldysh oscillations[7,8] appear which may be analyzed[9-13] accurately[14] to give the interband reduced masses at the critical point. The polarization dependence of these spectra gives in principle the symmetry of the critical point for nondegenerate bands,[15-18] and the relative contributions of the sub-bands if orbital degeneracies are involved.[19,20]

Ge is a classic "textbook" semiconducting material, being cubic, having inversion symmetry, and having well-separated critical-point transitions. In this paper, we summarize and extend our previous Schottky-barrier measurements on Ge[1,5,6,13,21] with the objective of obtaining accurate values of critical-point energies, broadening parameters, and interband reduced masses. We investigate polarization dependences, with particular emphasis on orbital degeneracies. We also investigate line-shape asymmetries to obtain information about the electron-hole interaction in the contact-exciton approximation.[22]

Our major conclusions, presented roughly in the order that they are discussed in the following sections, are as follows.

A. Theory

(i) The Stark shift for orbitally degenerate bands, such as the light-hole–heavy-hole degeneracy at $\vec{k}=0$, is significant only for energies

$$[E_{cv}(\vec{k})-E_g]\lesssim 4(\hbar\Omega)^3/E_g^2 ,$$

where $\hbar\Omega$ is the characteristic Franz-Keldysh energy [see Eq. (6)] and E_g is the critical-point energy. This quantity is of the order of fractions of an meV for Ge, so the Stark shift is completely negligible for most purposes.

(ii) The Keldysh-Konstantinov-Perel' (KKP) approximation,[19] derived initially for light-hole (lh) electroabsorption, applies within the same assumptions to heavy-hole (hh) spectra and to Franz-Keldysh oscillations in ER. The KKP approximation is potentially a great simplification because it enables one to calculate ER spectra of orbitally de-

generate critical points by (a) evaluating independently the, e.g., light- and heavy-hole contributions by nondegenerate theory; (b) calculating the matrix elements from $\vec{k}\cdot\vec{p}$ theory with $\vec{k}\parallel\vec{\mathcal{E}}$ and $\vec{\mathcal{E}}\to 0$; and (c) adding the results. Expressions for calculating the light- and heavy-hole matrix elements are obtained [Eqs. (16)]. The KKP approximation probably will *not* apply to low-field spectra. See also conclusions (iv)–(vi) below.

B. Experiment

(iii) The line-shape asymmetry of the low-field E_0 and $E_0+\Delta_0$ structures is accurately described using a two-dimensional model density of states to represent the unperturbed dielectric function, and using the generalized Seraphin coefficients[23] to calculate $\Delta R/R$. The amplitudes observed for intermediate-field spectra are in good agreement with calculated values. These results, together with the $\pm 10\%$ absolute-amplitude agreement previously obtained[24] in a simpler (electrolyte ER) configuration, demonstrate that the convolution-integral[25,26] or third-derivative approach is valid to describe continuum states even when relatively strong Coulomb effects may be present.

(iv) The KKP prediction of a linear superposition of nondegenerate spectra for orbitally degenerate critical points is verified for the E_0 transition. We extract explicitly the light- and heavy-hole ER spectra from the polarization data, and find a mass ratio 1.84 in acceptable agreement with theory[27] (1.74). A mass ratio of 1.73 was obtained by Handler *et al.*[11] by analyzing room-temperature ER spectra.

(v) The amplitude of the light-hole spectrum is observed to be 1.24 times larger (KKP prediction: 1.50) for [001] polarization relative to $[1\bar{1}0]$ polarization. The amplitude of the heavy-hole spectrum is observed to be 1.44 times larger (KKP prediction: 1.14) for $[1\bar{1}0]$ polarization relative to [001] polarization. Thus the KKP approximation predicts polarization anisotropies in ER in qualitative agreement with these experiments.

(vi) If the matrix-element magnitudes predicted by the KKP approximation are quantitatively correct, then the density-of-states prefactor is observed to be three times larger for light holes than heavy holes. This is clearly wrong. But we find that the *total* amplitude observed is in excellent agreement with theory. It follows that substantial matrix-elements mixing must occur in the exact solution which is not described in the KKP approximation, or else the light- and heavy-hole densities of states do not scale with mass as expected at orbitally degenerate critical points.

(vii) The width of the negative cusp in the E_0 spectrum is less than 2 meV at the highest fields attainable (115 kV cm^{-1}), for which $\hbar\Omega\cong 40$ meV. Thus the prediction of the simple theory of a functional singularity at threshold is verified remarkably well.

(viii) The low-field polarization anisotropies of the E_1 and $E_1+\Delta_1$ critical-point spectra are 1.32 ± 0.02 at 300 K and 1.20 ± 0.02 at 10 K, in excellent agreement with the values previously obtained[2] for GaAs. The theoretical value is $\frac{4}{3}=1.333\ldots$. The Coulomb interaction may cause this by reducing the anisotropy of the interband reduced mass. But the lower anisotropy could also result if the low-mass component is anomalously large, as suggested by the light- and heavy-hole interference in the Franz-Keldysh oscillations at intermediate fields.

(ix) The asymmetries of the E_1 and $E_1+\Delta_1$ line shapes are approximately those of two-dimensional and three-dimensional M_1 simple parabolic densities of states, respectively. Alternatively, the E_1 line shape could be interpreted as a three-dimensional M_0 threshold with a substantial Coulomb interaction. But the line shapes basically are too complicated to be given by simple parabolic-model densities of states, suggesting more elaborate models are required.[28]

(x) The E_0' triplet shows significant (and field-dependent) polarization anisotropies. At 115 kV cm^{-1}, the values of the anisotropies from peak-to-peak measurements for the E_0', $E_0'+\Delta_0'$, and $E_0'+\Delta_0+\Delta_0$ structures are 0.87, 1.39, and 0.82, respectively, for polarization $\hat{e}\parallel[1\bar{1}0]$ vs $\hat{e}\parallel[001]$. Anisotropy is expected within the KKP approximation,[19] but not within the simple theory. These results differ from previous (less-sensitive) transverse ER spectra[29] obtained for these transitions, where no critical-point anisotropy was observed. These results clearly indicate that symmetry analysis based on ER-spectra-polarization dependences alone should be treated with caution unless a critical point is known to be simple. (This does not imply that all spectral features whose polarization dependences are not simple arise from orbitally degenerate critical points.)

(xi) Matrix elements appear to be larger for light-hole transitions for E_0' and $E_0'+\Delta_0'+\Delta_0$, and for heavy-electron–hole transitions for $E_0'+\Delta_0'$. This follows from the Franz-Keldysh oscillations observed for these transitions. The heavy-electron–heavy-hole critical point is either of the M_1 type or has a relatively large electron-hole interaction.

(xii) Superposition of light/heavy electron/hole line shapes prevents interband reduced masses to be determined for E_0', $E_0'+\Delta_0'$, and $E_0'+\Delta_0'+\Delta_0$ transitions for $[1\bar{1}0]$, [001], and $[1\bar{1}0]$ polarizations, respectively. Masses determined for the other polarizations probably are light, heavy, and light reduced masses, respectively.

(xiii) The [001] spectra are 1.85 times larger than the $[1\bar{1}0]$ spectra for the E_2 transitions for low

TABLE I. Critical-point parameters for Ge, determined from Schottky-barrier ER measurements. The phase-angle errors $\Delta\theta$ were determined from two-dimensional M_0 model lineshapes and the Seraphin coefficients of the vacuum-Ni-Ge system given in Fig. 1.

Transition	E_g (meV)	Γ (meV)	$\Delta\beta$ (deg)	$\mu_{\parallel}$ (m_e) expt	$\mu_{\parallel}$(m_e) th
E_0(lh)	887.2±1	<1.8	−2	0.018±0.002	0.0200[a]
E_0(hh)	(889.2)[b]	(<0.5)[c]		0.0336±0.013	0.0346[a]
$E_0+\Delta_0$	1184±2	<24	0	0.0269[d]	0.0269[e]
E_1	2250±2	27	−10	(μ_T) 0.045±0.004	0.049[f]
$E_1+\Delta_1$	2434±2	44	+50	(μ_T) 0.042±0.005	0.050[f]
E_0'	3006±5	33	75	[001] 0.034±0.005	···
$E_0'+\Delta_0'$	3206±5	33	55	[1$\bar{1}$0] 0.048±0.009	···
$E_0'+\Delta_0'+\Delta_0$	3502±5	43	90	[001] 0.062±0.006	···
E_2	4501±10	66	220	0.139±0.015	0.12[g]
E_1'	5576±15	94	240	···	···
$E_1'+\Delta_1'$	5842±15	110	240	···	···
$E_1'+\Delta_1'+\Delta_1''$	6070±20	70(?)	240(?)	···	···

[a]From Eq. (16d), using the Luttinger parameters and conduction-band mass given by Lawaetz (Ref. 27).

[b]Probable best value, from 20-K absorption measurements by Macfarlane *et al.* (Ref. 43).

[c]From low-field data on relatively pure ($N_D \sim 7\times10^{13}$ cm^{-3}) sample by Bordure *et al.* (Ref. 54).

[d]Value fixed to give agreement to theoretical value. This fixes N_D and scales all values in this column.

[e]From Lawaetz (Ref. 27).

[f]From Dresselhaus and Dresselhaus (Ref. 62).

[g]Calculated from two-band model; see text.

fields. The large anisotropy, greater than $\frac{3}{2}$, proves that the critical point(s) responsible must have interband reduced masses of both signs. But the observation of Franz-Keldysh oscillations extending to higher energies[13] proves that the positive interband reduced-mass component(s) must be smaller than the negative interband reduced-mass component(s).

(xiv) The E_1' structures can be resolved into a triplet. The energy separation of the lower two structures is 266±10 meV, considerably more than the spin-orbit splitting $\Delta_1 = 184\pm2$ meV of the valence bands giving rise to the E_1 structure. This indicates that the critical points responsible are not the same for the two sets of structure.[21] This conclusion has been supported[30] by thermoreflectance measurements[31] on other semiconductors, and by synchrotron-radiation ER measurements also on Ge,[32] and on GaAs.[33]

(xv) Energies, broadening parameters, and lineshape asymmetries have been determined for all critical points observed to 6.2 eV. These quantities are given in Table I, together with interband reduced-mass values obtained from Franz-Keldysh oscillations. Spin-orbit and related splittings are given in Table II.

II. EXPERIMENT

All data reported here were taken on an n-type Ge crystal with $N_D = 6.4\times10^{15}$ cm^{-3}. This impurity concentration is very near the optimum value[5] where field-inhomogeneity effects[34] are minimized, yet reasonable electric fields are obtained. The [110] surface orientation used for these measurements provides the maximum possible data available in a surface-barrier geometry.[2] After Syton polishing, semitransparent Ni films were evaporated on these surfaces to form Schottky barriers for modulation purposes. Full details of the sample-fabrication process and the experimental ap-

TABLE II. Spin-orbit or other splittings determined from Schottky-barrier ER data given in Table I.

Splitting	Δ(meV)
$\Delta_0(E_0)$	287±1
Δ_1	184±2
$\Delta_0(E_0')$	296±3
Δ_0'	200±3
Δ_1'	266±10
Δ_1''	228±20

paratus have been given elsewhere.[2,35] Data were obtained in both low- and intermediate-field[36,37] limits.

III. THEORY

A. ER at orbitally degenerate critical points

Of the 11 structures investigated here, four (E_0, E_0', $E_0'+\Delta_0$, and $E_0'+\Delta_0+\Delta_0'$) are zone-center critical points involving bands with orbital degeneracy. Orbital degeneracies can cause large polarization anisotropies[19] (in the one-electron approximation) because the linear combinations of the degenerate wave functions that diagonalize the Hamiltonian are modified by the applied field.[17,19,20] Since the simple theory[8,25] deals only with nondegenerate wave functions, no such mechanism is included, and the simple theory predicts that zone-center critical points should show *no* polarization effects. This is not in agreement with previous measurements,[9,38] nor with our present data.

An approximate theory that describes the effects of orbital degeneracy on electroabsorption of light holes by field effects on the linear combinations has been given by KKP,[19] and numerical results have been given by Enderlein.[20] Here, we show that the KKP assumptions, made initially for light-hole exponential-edge electroabsorption,[19] are equally valid (or invalid) with respect to Franz-Keldysh oscillations seen in ER. We make the necessary (essentially trivial) extensions that enable us to interpret our ER data for both light and heavy poles within the KKP approximations.

The unperturbed Hamiltonian at $\vec{k}=0$ is

$$H_0 = p^2/2m + V(\vec{x}) + (\text{s.o.}) , \tag{1}$$

where $V(\vec{x})$ is the crystal potential and (s.o.) is the spin-orbit splitting. If we choose as a basis the states transforming as x, y, and z, then the $|\frac{3}{2}, m_j\rangle$ states at energy $E=0$ (the top of the valence band) that diagonalize H_0 are given by[39]

$$|\tfrac{3}{2}\tfrac{3}{2}\rangle = (-|x\uparrow\rangle - i|y\uparrow\rangle)/\sqrt{2} , \tag{2a}$$

$$|\tfrac{3}{2}\tfrac{1}{2}\rangle = (-|x\downarrow\rangle - i|y\downarrow\rangle + 2|z\uparrow\rangle)/\sqrt{6} , \tag{2b}$$

$$|\tfrac{3}{2}-\tfrac{1}{2}\rangle = (|x\uparrow\rangle - i|y\uparrow\rangle + 2|z\downarrow\rangle)/\sqrt{6} , \tag{2c}$$

$$|\tfrac{3}{2}-\tfrac{3}{2}\rangle = (|x\downarrow\rangle - i|y\downarrow\rangle)/\sqrt{2} , \tag{2d}$$

where the arrows represent the spin state. The lowest conduction band at $\vec{k}=0$ is represented by the symmetric states $|s\uparrow\rangle$ and $|s\downarrow\rangle$.

The orbital degeneracy is lifted by the $\vec{k}\cdot\vec{p}$ perturbation for $k=|\vec{k}|\neq 0$, and by the field perturbation $e\vec{\mathcal{E}}\cdot\vec{x}$ for $\mathcal{E}=|\vec{\mathcal{E}}|\neq 0$. The total perturbation is

$$H' = (\hbar/m)\vec{k}\cdot\vec{p} + e\vec{\mathcal{E}}\cdot\vec{x} . \tag{3}$$

We show first that the interband contribution of $e\vec{\mathcal{E}}\cdot\vec{x}$, the Stark shift,[40] is negligible compared to the $\vec{k}\cdot\vec{p}$ interaction for our measurements. It follows that only the intraband contribution of $e\vec{\mathcal{E}}\cdot\vec{x}$, the acceleration, is significant, and that ER can be described using the standard $\vec{k}\cdot\vec{p}$ band structure[41] calculated for orbitally degenerate critical points.

To prove this, we note that H' enters second-order degenerate perturbation theory[42] according to the square of matrix elements of the form

$$\langle s\uparrow | H' | x\uparrow\rangle = (\hbar/2m)kp_{cv} + e\mathcal{E}x_{cv} , \tag{4}$$

where $p_{cv}=\langle s\uparrow | p_x | x\uparrow\rangle$, $x_{cv}=\langle s\uparrow | x | x\uparrow\rangle$, and for simplicity we take $\vec{k}$, $\vec{\mathcal{E}} \parallel \hat{x}$. Clearly, the Stark shift will be negligible if $e\mathcal{E}x_{cv} < \hbar k p_{cv}/2m$. Now $x_{cv} = \hbar p_{cv}/mE_g$, where E_g is the fundamental direct gap, which follows by taking the matrix element of the commutator $[\vec{x}, H_0] = i\hbar\vec{p}$.

Putting the inequality in familiar terms we find that the Stark shift is negligible if

$$\hbar^2k^2/2\mu = E_{cv}(\vec{k}) - E_g > 4(\hbar\Omega)^3/E_g^2 , \tag{5}$$

where $\hbar\Omega$ is the characteristic Franz-Keldysh energy defined by

$$(\hbar\Omega)^3 = e^2\mathcal{E}^2\hbar^2/8\mu_{\parallel} \tag{6}$$

and $\mu_{\parallel}$ is the interband reduced mass in the field direction. For the highest fields attained here ($\mathcal{E}=115$ kV/cm), $\hbar\Omega=40$ meV for light holes [$\mu \cong 0.020m_e$ (Ref. 27)]. Since $E_g=889.2$ meV,[43] the right-hand side of Eq. (5) is 0.3 meV. Thus the Stark shift is important only within 0.3 meV of the critical-point energy. But this is totally negligible on our energy scale, and we conclude that Stark shift effects can be neglected.

We next investigate the KKP[19] assumptions with respect to heavy holes, and also to Franz-Keldysh oscillations in ER. The KKP approximation would enable one to calculate ER spectra at orbitally degenerate critical points quite simply by (a) calculating independently the light- and heavy-hole contributions by the nondegenerate theory, where (b) the matrix elements are those calculated from $\vec{k}\cdot\vec{p}$ theory with $\vec{k}\parallel\vec{\mathcal{E}}$ and $\vec{\mathcal{E}}\to 0$, and (c) adding the results.

The general $\vec{k}\cdot\vec{p}$ Hamiltonian for the states $|jm_j\rangle$ for $j=\frac{3}{2}$ is a 4×4 matrix.[44] If a_{mj} are the coefficients of the states $|\frac{3}{2}, m_j\rangle$ in a linear combination, then with intraband acceleration included the a_{mj} satisfy the Hamiltonian equations[44]

$$0 = (H_{11} + ie\vec{\mathcal{E}}\cdot\nabla_k + W)a_{3/2} + H_{12}a_{1/2} + H_{13}a_{-1/2} , \tag{7a}$$

$$0 = H_{12}^*a_{3/2} + (H_{22} + ie\vec{\mathcal{E}}\cdot\nabla_k + W)a_{1/2} + H_{13}a_{-3/2} , \tag{7b}$$

$$0 = H_{13}^*a_{3/2} + (H_{22} + ie\vec{\mathcal{E}}\cdot\nabla_k + W)a_{-1/2} - H_{12}a_{-3/2} , \tag{7c}$$

$$0 = H_{13}^*a_{1/2} - H_{12}^*a_{-1/2} + (H_{11} + ie\vec{\mathcal{E}}\cdot\nabla_k + W)a_{-3/2} , \tag{7d}$$

where

$$H_{11} = (\hbar^2/2m)[k^2(\gamma_1+\gamma_2) - 3k_z^2\gamma_2] , \tag{8a}$$

$$H_{12} = (\hbar^2/2m)[-2\sqrt{3}k_z(k_x - ik_y)\gamma_3] , \tag{8b}$$

$$H_{13}=(\hbar^2/2m)[\sqrt{3}\,(-k_x^2+k_y^2)\gamma_2+i2\sqrt{3}\,k_xk_y\gamma_3]\,, \quad (8c)$$

$$H_{22}=(\hbar^2/2m)[k^2(\gamma_1-\gamma_2)+3k_z^2\gamma_2]\,, \quad (8d)$$

$$k^2=k_x^2+k_y^2+k_z^2\,, \quad (8e)$$

and where the Luttinger parameters are defined by[44]

$$\gamma_1=\frac{2}{3m}\sum_\nu \frac{|\langle x|p_x|\nu\rangle|^2+2|\langle x|p_y|\nu\rangle|^2}{E_v+\frac{1}{3}\Delta-E_\nu}\,, \quad (9a)$$

$$\gamma_2=\frac{1}{3m}\sum_\nu \frac{|\langle x|p_x|\nu\rangle|^2-|\langle x|p_y|\nu\rangle|^2}{E_v+\frac{1}{3}\Delta-E_\nu}\,, \quad (9b)$$

$$\gamma_3=\frac{1}{3m}\sum \frac{\langle x|p_x|\nu\rangle\langle\nu|p_y|y\rangle+\langle y|p_x|\nu\rangle\langle\nu|p_y|x\rangle}{E_v+\frac{1}{3}\Delta-E_\nu}\,. \quad (9c)$$

If $\mathcal{E}=0$, then the energies of the light- and heavy-hole sub-bands are

$$E_v(\vec{k})=-W$$
$$=-(\hbar^2/2m)\{k^2\gamma_1\pm 2[k^4\gamma_2^2+3(\gamma_3^2-\gamma_2^2)\times(k_x^2k_y^2+k_y^2k_z^2+k_z^2k_x^2)]^{1/2}\}\,, \quad (10)$$

where the upper and lower signs refer to light and heavy holes, respectively.

If orbital degeneracy were *not* present, the off-diagonal terms in Eqs. (7) would vanish and the set would reduce to four independent first-order equations, which can be solved to obtain the field-dependent dielectric function in convolution form[25]:

$$\epsilon(E,\Gamma,\vec{\mathcal{E}})=1+\sum_{c,v}[\epsilon_{cv}(E,\Gamma,\vec{\mathcal{E}})+\epsilon_{cv}^*(-E,\Gamma,\vec{\mathcal{E}})]\,, \quad (11a)$$

$$\epsilon_{cv}(E,\Gamma,\vec{\mathcal{E}})=[ie^2\hbar^2/\pi^2m^2(E+i\Gamma)^2]\times\int_{BZ}d^3k\int_0^\infty ds\,[\hat{e}\cdot\vec{p}_{vc}(\vec{k}-\tfrac{1}{2}e\vec{\mathcal{E}}s)][\hat{e}\cdot\vec{p}_{cv}(\vec{k}+\tfrac{1}{2}e\vec{\mathcal{E}}s)]\times\exp\left\{i\int_{-s/2}^{s/2}ds'[E+i\Gamma-E_{cv}(\vec{k}-e\vec{\mathcal{E}}s')]\right\}\,, \quad (11b)$$

where

$$E_{cv}(\vec{k})=E_c(\vec{k})-E_v(\vec{k})\,.$$

It would appear that Eqs. (7) can be decoupled by a transformation matrix to remove the off-diagonal components of the Hamiltonian matrix. This is generally not possible, because the form of the intraband operator $ie\cdot\nabla_k$ in Eqs. (7) is obtained by assuming that the periodic parts of the Bloch functions $|j,m_j\rangle$ are only weakly dependent on $\vec{k}$. In this case

$$\vec{x}|j,m_j\rangle\cong -i\nabla_k|j,m_j\rangle\,. \quad (12)$$

Since the H_{ij} are dependent on $\vec{k}$, the a_{mj} are dependent on $\vec{k}$, and Eq. (12) does not hold for a general linear combination $\sum_{mj}a_{mj}|j,m_j\rangle$. Then the coupling terms cannot vanish, and a numerical solution[20] is required.

But KKP[19] have pointed out that since the a_{mj} depend only on the *direction* of $\vec{k}$ and not on its magnitude, decoupling occurs if in effect $|\frac{1}{2}e\vec{\mathcal{E}}s|\gg|\vec{k}|$ in Eq. (11b) for the region of contribution to the integral. This was proven to be the case for light-hole electroabsorption,[19] by making tacitly the additional assumption that the initial values of the coefficients a_{mj}, determined by taking $\vec{k}\parallel\vec{\mathcal{E}}$, would not change by evolution as described by Eqs. (7). If this is the case, then Eqs. (7) decouple since $\vec{\mathcal{E}}\cdot\nabla_k a_{mj}(\vec{k}_\parallel)=0$, where $\vec{k}_\parallel=\vec{k}\parallel\vec{\mathcal{E}}$. This important simplification enables one to calculate field effects as a linear superposition of solutions of the form of Eq. (11a), with each hole accelerating according to its mass calculated from Eq. (10) with $\vec{k}=\vec{k}_\parallel$. The only significant change relative to the nondegenerate case is that the matrix element in Eq. (11a) must be calculated from the appropriate linear combination obtained from Eqs. (7), (8), and (10) for $\vec{k}=\vec{k}_\parallel$, and that this matrix element depends upon the direction of $\vec{\mathcal{E}}$.

We adapt the KKP approximation to ER by noting that $|\frac{1}{2}e\vec{\mathcal{E}}s|\gg|\vec{k}|$ for heavy holes as well as light holes, and for Franz-Keldysh oscillations as well as exponential-absorption edges, for zone-center orbitally degenerate critical points. We have shown[14] that ER spectra can be separated into two principal components: a low-field contribution originating near $s=0$ and an oscillatory (or exponential-edge) contribution originating near

$$s^2=s_0^2\cong[E-E_{cv}(\vec{k})]/(\hbar\Omega)^3\,. \quad (13)$$

Now the inequality $|\frac{1}{2}e\vec{\mathcal{E}}s_0|\gg|\vec{k}|$ clearly does not apply to the low-field contribution originating near $s=0$. It may or may not apply to the oscillatory contribution depending upon the range of $|\vec{k}|$ important to Eq. (11b). But we have also shown[14] that the dominant contribution to the Brillouin-zone integral over $\vec{k}$ extends from $\vec{k}=0$ to about

$$k_{max}^2\cong(2\mu/\hbar^2)(E-E_g)^{1/2}/(\hbar\Omega)^{3/2}\,. \quad (14)$$

Transforming Eqs. (13) and (14) to familiar terms, we find that the condition $|\frac{1}{2}e\vec{\mathcal{E}}s_0|\gg|\vec{k}|$ is satisfied if

$$E-E_g>|\hbar\Omega|\,. \quad (15)$$

This is a less-stringent condition than that required by the asymptotic expansion itself. Thus we conclude that the KKP approximation is as applicable to Franz-Keldysh oscillations as it is to exponential absorption edges.

By using Eqs. (7), (8), and (10) in the limit that $\vec{\mathcal{E}}\to 0$ and $\vec{k}\parallel\vec{\mathcal{E}}$, one can evaluate the sums over initial light- or heavy-hole valence states and the conduction-band final states in the KKP approximation. We find that

$$\sum_{v,c} |\hat{e}\cdot\vec{p}_{cv}|^2|_{\vec{k}_\parallel} = p_{cv}^2\left(\frac{2}{3} - \frac{\gamma_2}{3g(\hat{\epsilon})}[1-3(\hat{e}\cdot\hat{\mathcal{E}})^2] + \frac{2(\gamma_3-\gamma_2)}{g(\hat{\epsilon})}(e_x e_y \hat{\mathcal{E}}_x\hat{\mathcal{E}}_y + e_y e_z \hat{\mathcal{E}}_y\hat{\mathcal{E}}_z + e_z e_x \hat{\mathcal{E}}_z\hat{\mathcal{E}}_x)\right), \quad (16a)$$

where p_{cv} is defined following Eq. (4), γ_2 and γ_3 are the Luttinger parameters, $\hat{e}$ is the polarization vector, $\hat{\mathcal{E}} \parallel \vec{\mathcal{E}}$ and $\hat{\mathcal{E}}_x^2 + \hat{\mathcal{E}}_y^2 + \hat{\mathcal{E}}_z^2 = 1$, and

$$g(\hat{\epsilon}) = \pm[\gamma_2^2 + 3(\gamma_3^2 - \gamma_2^2)(\hat{\mathcal{E}}_x^2\hat{\mathcal{E}}_y^2 + \hat{\mathcal{E}}_y^2\hat{\mathcal{E}}_z^2 + \hat{\mathcal{E}}_z^2\hat{\mathcal{E}}_x^2)]^{1/2}, \quad (16b)$$

where the positive sign refers to light holes and the negative sign to heavy holes. The energies $E_v(\vec{k})$ and the effective masses in the field direction are given by

$$E_v(\vec{k}) = -(\hbar^2k^2/2m)[\gamma_1 + 2g(\hat{\epsilon})], \quad (16c)$$

$$m_e/m^*_{l,h} = -\gamma_1 - 2g(\hat{\epsilon}). \quad (16d)$$

The light-hole expressions are identical to those previously obtained by KKP.[19] The only difference is that $g(\hat{\epsilon})$ is negative instead of positive for heavy holes. In the KKP approximation, Eqs. (16) are to be used in evaluating Eqs. (11).

B. Energy gaps, broadening parameters, and line-shape asymmetries

ER line shapes are given by[5]

$$\frac{\Delta R}{R} = \mathrm{Re}[(Ce^{i\Delta\theta})\tilde{C}_s\tilde{C}_{ex}\tilde{C}_{in}e_ie_j\Delta\epsilon^{ij}(E,\Gamma,\vec{\mathcal{E}})] + A + B(E-E_g). \quad (17)$$

In Eq. (17), we have included $Ce^{i\Delta\theta}$ to measure any discrepancies between theory (the rest of the bracketed quantity) and experiment. $\tilde{C}_s$ is the complex Seraphin coefficient, whose value we have calculated as a function of E for our system.[23] We shall only use the phase, which is given in Fig. 1. $\tilde{C}_{ex}$ is the contact exciton parameter[22]

$$\tilde{C}_{ex} = [1 + g(\epsilon - 1)]^2, \quad (18)$$

where the strength parameter $g \lesssim 0$. $\tilde{C}_{in}$ is the field-inhomogeneity factor[34] which is small for depletion regions[34,45] and will be neglected. The constants A and B compensate for possible slowly varying backgrounds, and $\Delta\epsilon(E,\Gamma,\vec{\mathcal{E}})$ is the field-dependent part of Eq. (11a).

At low fields in the parabolic-band approximation,[4]

$$e_ie_j\Delta\epsilon^{ij} \propto (\hbar\Omega)^3|\hat{e}\cdot\vec{p}_{cv}|^2\exp[i\tfrac{1}{2}\pi(2-D)] \times (E-E_g+i\Gamma)^{-(4-D/2)}, \quad (19)$$

where $D = 1, 2, 3$ is the critical-point dimension and $l = 0, 1, 2, 3$ is the critical-point type. At intermediate fields the closed-form solutions[8] are needed for the complete description but the oscillatory part is given approximately by[14]

$$e_ie_j\Delta\epsilon^{ij} \propto E^{-2}(E-E_g)^{-1}\exp[-(E-E_g)^{1/2}\Gamma/(\hbar\Omega)^{3/2}] \times \cos\{\theta + \tfrac{2}{3}[(E-E_g)/\hbar\Omega]^{3/2}\}, \quad (20)$$

where θ is an adjustable parameter.

Energy gaps, broadening parameters, and asymmetries are obtained from low-field spectra by fitting Eq. (17) to the data using Eq. (19) to represent $\Delta\epsilon$. This is an extension of the three-point method[46] which gives more equal weighting to the individual points. Interband reduces masses are obtained from the energies E_v of successive tangent points between Eq. (20) and its envelope by the slope analysis described previously.[2,13]

The electron-hole interaction is included only qualitatively in Eq. (18). Calculations of field effects including the Coulomb interaction are presently available only in numerical form,[47,48] so a detailed comparison in not practical. But we have shown that the convolution-integral approach[25,26] (which is equivalent to taking the third derivative of the *measured* dielectric function) gives quantitative agreement to within 10% for the E_0 edge at 300 K,[24] and that the direct third-derivative approach gives agreement to within 40% for E_1 and $E_1+\Delta_1$ transitions.[6] Therefore, we shall include the Coulomb interaction approximately by using two-dimensional model densities of states instead of three-dimensional, in agreement with line-shape calculations of the Coulomb continuum threshold.[49] While not exact, we shall show that this approach yields line-shape asymmetries in good agreement with experiment for low-energy critical points.

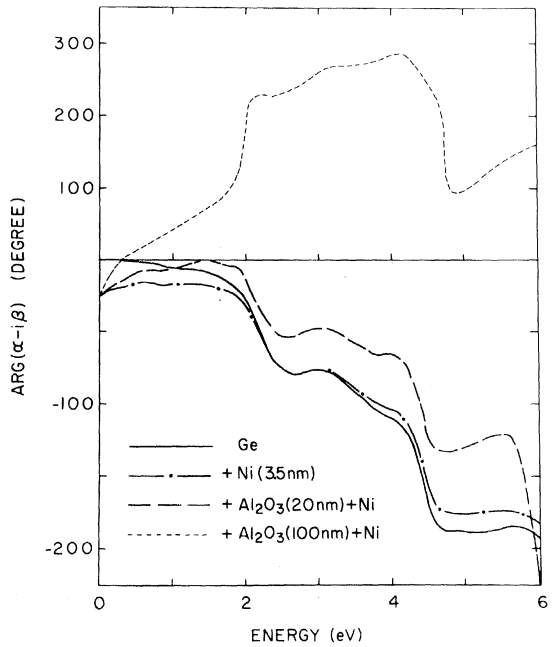

FIG. 1. Phase of the complex Seraphin coefficients for the Ge-Ni system (after Ref. 23).

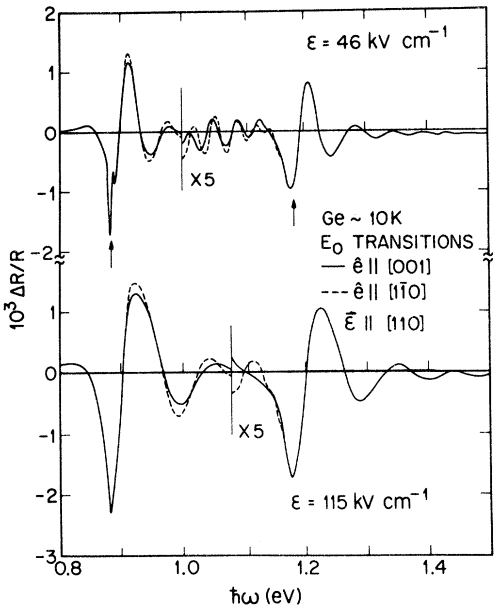

FIG. 2. Representative Schottky-barrier ER spectra of the E_0 and $E_0+\Delta_0$ critical points of Ge at 10 K. The field $\vec{\mathcal{E}} \parallel [110]$. Spectra for $\hat{e} \parallel [001]$ (——) and $\hat{e} \parallel [1\bar{1}0]$ (- - - - -) are given for two intermediate values of $\mathcal{E}$. Critical-point energies are indicated by arrows in the upper curves.

IV. RESULTS AND DISCUSSION

A. $E_0, E_0+\Delta_0$ transitions

1. Critical-point energy, broadening parameter, and line-shape asymmetry

Spectra for the E_0 and $E_0+\Delta_0$ transitions at two intermediate field values are shown in Fig. 2. Structure due to field ionization of the $n=1$ exciton line can be seen clearly near the negative extremum of the principal structure of the E_0 transition in the upper curve. It has the expected line shape of the negative of the dispersion curve, but in general the shape is not invariant due to interference with the reflected intensity from the optical discontinuity formed at the back of the Schottky barrier. For example, the line shape of the $n=1$ line in Ge is inverted on the equivalent spectrum shown in Fig. 1 of Ref. 13, which was obtained at a slightly lower value of the modulating field. The inversion effect has previously been studied in other materials.[2,50,51]

As in GaAs,[2] we have been unable to reach low enough fields with $N_D \sim 10^{16}$ cm^{-3} to obtain true low-field ER spectra for either the E_0 or $E_0+\Delta_0$ transition at low temperature. But the energy gap and broadening parameter for E_0 can be obtained from the $n=1$ exciton structure. Using a Lorentzian-model line shape [$D=6$ in Eq. (19)], we find $E_{ex} = 885.8 \pm 0.5$ meV and $\Gamma = 1.8 \pm 0.3$ meV. We obtain the critical-point energy in Table I by adding the average of the binding energies of the light- and heavy-hole excitons.[47] The exciton energy is somewhat lower than that obtained by Nishino *et al.* in electroabsorption measurements at very low fields (889.0 meV at 24 K at 600 V cm^{-1})[52] and that obtained by Macfarlane *et al.*[43] in absorption measurements (889.2 meV at 20 K). But in ER measurements using a SnO_2-Ge heterojunction configuration, Nishino and Hamakawa[12] found a substantially lower value for the critical-point energy (879 meV at 24 K at 9 kV cm^{-1}).[53] A somewhat lower value was also found by Bordure *et al.*,[54] with a Cu_2S heterojunction to a relatively pure ($N_D \cong 7 \times 10^{13}$ cm^{-3}) Ge crystal. Applying the three-point method to their data, we find the exciton peak at 887 ± 0.5 meV with a broadening parameter of about 0.5 meV. This leads to critical-point energy of about 888.5 meV. The slightly lower value that we obtain is consistent with results obtained for GaAs, where the exciton energy is observed to shift to lower energies with increasing impurity concentration.[55]

The exciton structure could not be resolved for the $E_0+\Delta_0$ transition. But the critical-point energy can be obtained by applying the three-point method to both E_0 and $E_0+\Delta_0$ structures, taking the difference between the calculated critical point energies to obtain the spin-orbit splitting, then adding the spin-orbit splitting to the critical-point energy determined from the exciton structure of E_0. We find

$$\Delta_0 = 1192.7 - 895.6 \text{ meV} = 297.1 \pm 1 \text{ meV},$$

yielding the value given in Table I. It was not possible to obtain a broadening parameter since low-field spectra could not be obtained for this transition. The minimum value observed, based on a two-dimensional (2D) model, was 24 meV. The spin-orbit splitting obtained here agrees well with the value 295 ± 3 meV obtained by Fischer[56] in transverse ER measurements on γ-ray compensated Ge at 85 K.

The asymmetry of the line shape determines the phase of the coefficient product in brackets in Eq. (17). Using the value of $\arg(C_s) = -17°$ from Fig. 1, taking $C_{ex} = C_{in} = 1$, and assuming a 2D M_0 model critical-point representative of the Coulomb continuum,[49] we find by the three-point method for the lowest-field spectrum that we could measure, with the exciton contribution removed, that $\theta = -2°$. Thus the 2D M_0 line shape completely accounts for the observed asymmetry. Since we have already demonstrated amplitude agreement in a physically simpler system,[24] the asymmetry result adds further evidence of the validity of the convolution[25,26] or third-derivative[4,6] approach for band-to-band transitions even in the presence of relatively strong electron-hole–interaction effects. The same excellent agreement is obtained for the $E_0+\Delta_0$ edge,

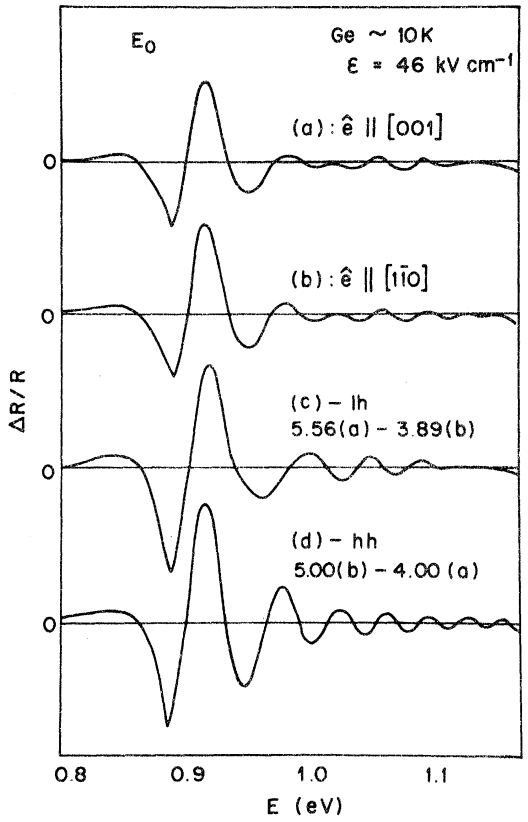

FIG. 3. Separation of 46-kV cm^{-1} E_0 spectra for (a) $\hat{e} \parallel [001]$; and (b) $\hat{e} \parallel [1\bar{1}0]$ into (c) light-hole and (d) heavy-hole components. The equations used to form the linear combinations are shown. The abscissa scale is relative. The light-hole spectrum has been scaled to have the same peak-to-peak amplitude as the heavy-hole spectrum, as if each were given by the same electro-optic (G) function.

where the three-phase correction of $-17°$ entirely accounts for the observed line-shape asymmetry.

At high fields, the line shapes evolve into those expected from numerical calculations,[47,48] and are similar in appearance to the G function of the one-electron approximation. It is remarkable that the negative cusp is less than 2 meV wide on a structure where the intrinsic energy scale $\hbar\Omega$ is 40 meV. This is a dramatic confirmation of the prediction of the simple theory of a functional singularity at threshold.

The energies of the negative extrema of the high-field E_0 and $E_0+\Delta_0$ structures are 883 and 1181 meV, respectively. If these are interpreted as the critical point energies, then they represent downshifts of 5 meV and 3 meV compared to the low-field values. This effect may be due to local heating from power (of the order of 10 mW) dissipated in the sample under high-field conditions. No remnant of the $n=1$ exciton line appears in these spectra.

2. Polarization effects, amplitudes, and selection rules

The KKP approximation predicts that the orbitally degenerate E_0 ER line shapes in Fig. 2 are *linear* combinations of nondegenerate light- and heavy-hole line shapes, with different weighting factors for $\hat{e} \parallel [001]$ and $\hat{e} \parallel [1\bar{1}0]$. This is also indicated by the interference pattern previously analyzed,[11] which is also seen in the oscillations of Fig. 2.

We obtained a striking verification of this prediction by finding linear combinations of the 46-kV cm^{-1} E_0 spectra of Fig. 2 that separate explicitly into light- and heavy-hole contributions, as shown in Fig. 3. (a) and (b) are copies of the 46-kV cm^{-1} spectra in Fig. 2. (c) and (d) were calculated by the linear combinations,

$$(\Delta R/R)_{\mathrm{lh}} = 5.56(\Delta R/R)_{001} - 3.89(\Delta R/R)_{1\bar{1}0}\,, \qquad (21a)$$

$$(\Delta R/R)_{\mathrm{hh}} = 5.00(\Delta R/R)_{1\bar{1}0} - 4.00(\Delta R/R)_{001}\,. \qquad (21b)$$

The relative values for each combination were chosen to give the best "separation" defined as giving the apparently smoothest decay envelope. The magnitudes for the heavy-hole coefficients were chosen simply to give unity net weight (a difference of 1.00). The magnitudes of the light-hole coefficients were chosen to give a peak-to-peak spectral amplitude equal to that for the heavy-hole spectrum. The assumption here, of course, is that the same *line-shape* mechanism is responsible for both. The uncertainty in each coefficient is about 5%.

To verify that these spectra indeed represented the light- and heavy-hole contributions, we plotted the tangent energies E_ν as $(E_\nu - E_g)^{3/2}$ vs ν as shown in Fig. 4, to obtain the slopes of the resulting straight lines. The square of the slope ratio, by Eqs. (6) and (20), gives an interband reduced-mass

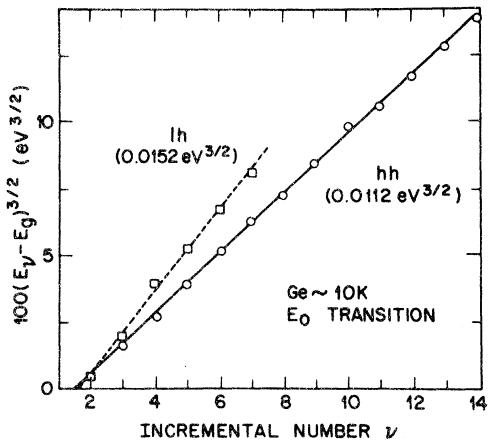

FIG. 4. Determination of interband reduced-mass ratio from the separated spectra of Fig. 3. The square of the ratio of the slopes given is 1.84, the theoretical value (see text) is 1.73.

ratio of the critical point as 1.84. Using the known[27] values $m_c^* = 0.038m_e$, $\gamma_1 = 13.35$, $\gamma_2 = 4.25$, and $\gamma_3 = 5.69$, we calculate from Eq. (16d) that for $\vec{\mathcal{E}} \parallel [110]$, $|g(\hat{\epsilon})| = 5.37$, and, finally, $m_{l\parallel}^* = -0.042m_e$, $m_{h\parallel}^* = -0.382m_e$. Therefore, $\mu_{l\parallel} = 0.0200m_e$ and $\mu_{h\parallel} = 0.0346m_e$.[57] The mass ratio obtained from theory is 1.73. Our experimental ratio of 1.84 is in acceptable agreement.

Equations (21) enable matrix-element ratios and density-of-states prefactors to be determined for the E_0 transition. We suppose that the same lineshape mechanism gives rise to both light- and heavy-hole spectra. Then we can write

$$(\Delta R/R)_{1h} = D_{1h}|\hat{e}\cdot\vec{p}_{cv}|_{1h}^2 G[(E-E_g)/\hbar\Omega_{1h}], \quad (22a)$$

$$(\Delta R/R)_{hh} = D_{hh}|\hat{e}\cdot\vec{p}_{cv}|_{hh}^2 G[(E-E_g)/\hbar\Omega_{hh}], \quad (22b)$$

where $G(x)$ is a universal electro-optic function, probably of a three-dimensional (3D) type (intermediate-field data). From Eqs. (16) and the Lawaetz[27] values of γ_1, γ_2, and γ_3, we find

$$(\Delta R/R)_{001} = 0.201D_{1h}P_{cv}^2G_{1h} + 0.465D_{hh}P_{cv}^2G_{hh}, \quad (23a)$$

$$(\Delta R/R)_{1\bar{1}0} = 0.134D_{1h}P_{cv}^2G_{1h} + 0.532D_{hh}P_{cv}^2G_{hh}. \quad (23b)$$

From experiment [Eqs. (21)],

$$(\Delta R/R)_{001} = 0.41(\Delta R/R)_{1h} + 0.32(\Delta R/R)_{hh} \quad (24a)$$

$$(\Delta R/R)_{1\bar{1}0} = 0.33(\Delta R/R)_{1h} + 0.46(\Delta R/R)_{hh}. \quad (24b)$$

Examination of Eqs. (23) and (24) shows that, with regard to polarization dependence, the KKP approximation is qualitatively correct since it predicts an increased heavy-hole contribution for $[1\bar{1}0]$ polarization. But the heavy-hole increase, predicted to be a factor of 1.14, is somewhat larger, 1.44. Also, the light-hole increase for [001] polarization, predicted to be 1.50, is smaller, 1.24. The discrepancy is outside experimental error. It may be due to our determining the height ratios near $E = E_g$, where the KKP approximation is probably not too accurate. The ratios of light- to heavy-hole contributions for a single polarization are 1.28 and 0.72 for [001] and $[1\bar{1}0]$, respectively. This is in good agreement with the previous results of Handler *et al.*,[11] who obtained 1.16 and 0.71, respectively, in fitting the interference of room-temperature electrolyte ER data.

If we assume that the KKP prediction is quantitatively correct, we can estimate the relative values of the light- and heavy-hole density of states prefactors from Eqs. (23) and (24). Averaging the results for the two polarizations gives

$$D_{1h}/D_{hh} = 2.9 \pm 20\%. \quad (25)$$

This is surprising, since in the intermediate-field limit the prefactor mass dependence should be proportional to μ^2 if Coulomb effects dominate or to $\mu^{4/3}$ if the three-dimensional model applies.[58] Thus one in fact expects the *opposite* behavior to that which is observed.

To see whether the *total* oscillator strength agrees with theory, even if the partial contributions are not in the correct proportion, we calculate the total amplitudes and compare to the results shown in Fig. 2. For a 3D M_0 threshold[8]

$$\Delta\epsilon_{cv} = \frac{ie^2\hbar^2|\hat{\epsilon}\cdot\vec{p}_{cv}|^2}{m^2\omega^2}\left(\frac{2\mu}{\hbar^2}\right)^{3/2}[G_3(x) + iF_3(x)], \quad (26)$$

where G_3 and F_3 are the three-dimensional electro-optic functions. Now for the 115-kV cm^{-1} spectrum, we are well above the limit[59] $\hbar\Omega \cong 10\Gamma$ for which broadening effects must be considered in the amplitude of F_3 and G_3. Therefore,[8] $G_3|_{pp} \cong 0.54$. Since for our configuration the generalized Seraphin coefficient amplitude at 0.90 eV is 0.0204,[23] the peak-to-peak amplitude of $\Delta R/R$ for either light- or heavy-hole transitions can be written from Eq. (26) and the above as

$$\left.\frac{\Delta R}{R}\right|_{pp} \cong 0.0204\frac{16\times 2^{1/3}R_y^{3/2}(\hbar\Omega)^{1/2}}{E^2} \times\left(\frac{\mu}{m_e}\right)^{3/2}\frac{|\hat{\epsilon}\cdot\vec{p}_{cv}|^2 a_B^2}{\hbar^2}G_3|_{pp}, \quad (27)$$

where $R_y = 13.6$ eV, $a_B = 0.529$ Å, and

$$|\hat{\epsilon}\cdot\vec{p}_{cv}| = P_{cv}/\sqrt{3} = 0.37/a_B$$

in the isotropic approximation. The numerical value for P_{cv} was obtained[24] by fitting the amplitude of the two-dimensional Coulomb continuum to the observed[43] absorption coefficient $\alpha = 3500$ cm^{-1} just above threshold. The prefactor 16 contains a factor of 2 for spin degeneracy. Using the above values, the field $\mathcal{E} = 115$ kV cm^{-1}, and the masses $\mu_{1h} = 0.018m_e$ and $\mu_{hh} = 0.0336m_e$ (see Sec. IV A 3), we calculate from Eq. (27) that

$$\Delta R/R|_{pp} = (1.0 + 2.2)\times 10^{-3} = 3.2\times 10^{-3}, \quad (28)$$

where the first and second values represent the light- and heavy-hole contributions, respectively, assuming equal matrix elements. Using the average weighting given by the KKP approximation, we find

$$\Delta R/R|_{pp} = (0.5 + 3.3)\times 10^{-3} = 3.8\times 10^{-3}. \quad (29)$$

By Fig. 2, the experimental value of $\Delta R/R|_{pp}$ averaged over both polarizations is 3.7×10^{-3}. Thus we see that the observed *total* amplitude is in excellent agreement with theory, but that the *individual* contributions are substantially different. It appears that the matrix-element magnitudes predicted by the KKP approximation are not correct, or else the density-of-states prefactors for these critical points are not simply proportional to the individual masses.

It is straightforward to repeat the above calculation for a two-dimensional Coulomb continuum, which has an amplitude

$$\Delta\epsilon = \frac{4\pi e^2 |\hat{\epsilon}\cdot\vec{p}_{cv}|^2}{m^2E^2}\frac{\mu^2}{K_0 m_e}(G_2+iF_2)$$
$$= \frac{32\pi}{K_0}\left(\frac{R_y}{E}\right)^2 \frac{|\hat{\epsilon}\cdot\vec{p}_{cv}|^2 a_B^2}{\hbar^2}\left(\frac{\mu}{m}\right)^2 (G_2+iF_2), \quad (30)$$

obtained by applying the convolution integral[25] to the density of states of the Coulomb continuum. Using the previous values and $G_2|_{pp} \cong 0.88$,[60] we calculate, using equal matrix elements, that

$$\Delta R/R|_{pp} \cong (0.7+2.1)\times 10^{-3} \cong 2.9\times 10^{-3}\ . \quad (31)$$

This is comparable to, but less than, the value obtained from the three-dimensional expression. It is clear that the rise in ϵ_2 that occurs as the energy increases would result in a larger estimate for the two-dimensional case. Thus either three-dimensional parabolic or two-dimensional Coulomb-continuum models should give good results in the intermediate-field limit as far as amplitudes are concerned.

3. *Interband reduced masses*

These were determined for the $E_{0,\mathrm{lh}}$ and $E_{0,\mathrm{hh}}$ transitions as discussed previously[13] by means of the slope analysis based on Eq. (20). We determined the mass scale by fixing the proportionality constant to make the $E_0+\Delta_0$ mass agree with the known value, $0.092m_e$.[27] The values obtained, $\mu_{\mathrm{hh}\parallel} = (0.0336\pm0.013)m_e$ and $\mu_{\mathrm{lh}\parallel} = (0.018\pm0.002)m_e$, are in good agreement with the values $\mu_{\mathrm{hh}\parallel} = 0.0346m_e$ and $\mu_{\mathrm{lh}\parallel} = 0.0200m_e$ obtained from Eq. (16d) and the conduction-band mass of $m_c^* = 0.038m_e$ given by Lawaetz.[27] The results are given in Table I.

B. E_1, $E_1+\Delta_1$ transitions

Spectra for the E_1 and $E_1+\Delta_1$ transitions for one low- and one intermediate-field value are shown in Fig. 5. The spectra for $\hat{e}\parallel[1\bar{1}0]$ have been scaled by factors of 1.20 and 1.18 for the low- and intermediate-field spectra, respectively, to show more clearly the basic line-shape similarities.

Since these structures originate with critical points of [111] symmetry,[61] a [110] field splits the eightfold degeneracy of the equivalent points of the star of $\vec{k}_c$ into two fourfold-degenerate sets making angles of 90° and 35.3° with the applied field. The nearly parallel bands along[62,63] [111] yield $|\mu_L| \gg \mu_T$, where μ_L and μ_T are the interband reduced masses parallel and perpendicular to the symmetry axis, respectively. Evaluating the matrix elements gives relative weights of 8 and 8 for [001] polarization, and 12 and 4 for $[1\bar{1}0]$ polarization, for the (nearly) longitudinal and the transverse sets, respectively.

The qualitative effect of degeneracy removal and matrix-element effects appears in the Franz-Keldysh oscillations above the main E_1 and main $E_1+\Delta_1$ structures. The oscillation period is shorter for $\hat{e}\parallel[1\bar{1}0]$, expected because the set with larger $\mu_\parallel$ (and smaller $\hbar\Omega$) is favored by a 3:1 matrix-element ratio. For $\hat{e}\parallel[001]$ the matrix element ratio is 2:2. The period appears to increase because of the heavier relative weight given to the transverse set. We have not attempted a separation of these data as with the E_0 results to obtain relative weightings, although there appears to be no fundamental reason why this could not be done with more complete data. The present data suggest—as with the E_0-edge results—that the light-mass component may be anomalously large.

In the simple theory with the low-field density-of-states prefactors in a 3:1 ratio [see Eq. (19)], the polarization anisotropy of the low-field spectra should be $(8+3\times8)/(12+3\times4) = 1.333$ ([001] larger). This is in qualitative agreement with Fig. 5, but we observe the anisotropy to be 1.20 ± 0.02. We performed room-temperature anisotropy measurements and found the room-temperature anisotropy to be 1.32 ± 0.02, in excellent agreement with the theoretical value. These results are in excellent agreement with our previous results on GaAs,[2] and show another effect becomes important as the broadening decreases.

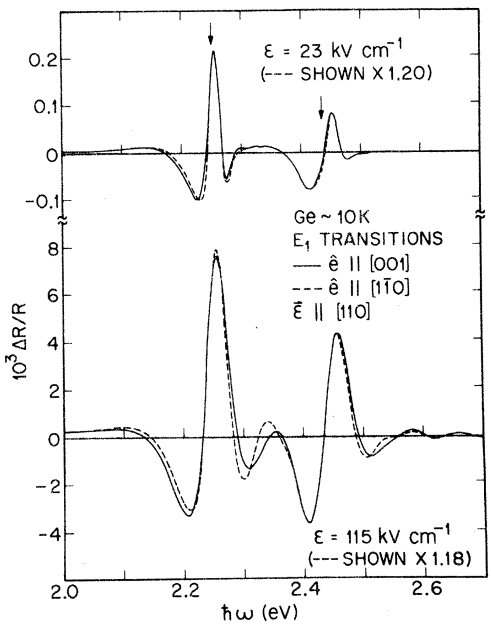

FIG. 5. Representative Schottky-barrier ER spectra of the E_1 and $E_1+\Delta_1$ critical points of Ge at 10 K. The field $\vec{\mathcal{E}}\parallel[110]$. Spectra for $\hat{e}\parallel[001]$ (——) and $\hat{e}\parallel[1\bar{1}0]$ (- - - -) are given for a low and an intermediate value of the field. Critical-point energies are indicated by arrows in the upper curves.

The (isotropic) Coulomb interaction may be responsible for decreasing the mass anisotropy at low temperature. But if the low-mass component is found to be anomalously large, the effect is easily understandable by matrix elements alone. If the low/high mass scaling is 2 instead of 3, the anisotropy becomes less: $(8+2\times8)/(12+2\times4) = 1.20$. If the two sets have the same amplitude the anisotropy disappears. Further measurements are needed to resolve this problem. Any explanation must also include the anomalously small anisotropy observed by Sari[64] in magnetoreflectance measurements.

The critical-point energies, broadening parameters, and asymmetries determined from a two-dimensional low-field model and the Seraphin coefficients in Fig. 1 are shown in Table I. The spin-orbit splitting, $\Delta_1 = 184 \pm 2$ meV, determined from these values is less than the value, 198 meV, predicted by the "two-thirds" rule from the value of Δ_0. The broadening of the $E_1+\Delta_1$ transition is apparently much larger than that of E_1. But it is clear that the line shapes are qualitatively different, and neither is sufficiently simple to suggest that they can be represented by a single parabolic critical point. This indicates that the detailed dependence of the interband energy on momentum along the symmetry axis must be included in any line-shape calculation for these transitions.[28]

Despite the line-shape differences, the generalized Seraphin coefficient and two-dimensional M_0 model density of states account well for the asymmetry of the E_1 transition. By contrast, the $E_1+\Delta_1$ transition has the asymmetry of a three-dimensional M_1 model density of states if Coulomb effects are ignored, or shows substantial Coulomb effects if a two-dimensional M_0 model is assumed. It is not clear why Coulomb effects should be more important for the higher-energy transition, where the broadening is larger.

Effective masses of the E_1 and $E_1+\Delta_1$ transitions were obtained from the $[1\bar{1}0]$ spectra as described earlier. Here, the light-mass component μ_T predominates. The results are shown in Table I and agree reasonably well with the calculated values of Dresselhaus and Dresselhaus.[62]

C. E_0' transitions

All E_0' transitions start and/or end on orbitally degenerate bands. A polarization dependence should be expected according to the KKP approximation. This is observed, as seen in Fig. 6. The two representative sets of intermediate-field spectra show much greater detail than previous E_0' ER results[1,21,29,56] for Ge. These data also provide the first evidence of polarization anisotropy in ER at E_0' transitions in Ge. Previous low-temperature surface-barrier ER data[2] were taken on

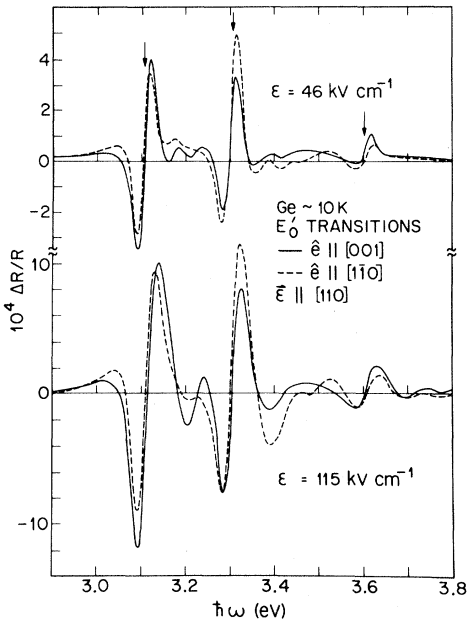

FIG. 6. Representative Schottky-barrier ER spectra of the E_0' triplet of Ge at 10 K. The field $\vec{\varepsilon} \parallel [110]$. Spectra for two intermediate values of the field are shown for polarizations $\hat{e} \parallel [001]$ (——) and $\hat{e} \parallel [1\bar{1}0]$ (- - - -). Critical-point energies are indicated by arrows in the upper curves.

{111} surfaces, for which a polarization dependence is not expected. Previous transverse ER data[29] either did not show an anisotropy or else were not taken with sufficient sensitivity to resolve it.

The KKP approximation[19] developed in Sec. III for the E_0 transition will not apply directly since the conduction-band basis here must be represented by states transforming as xy, yz, and zx, to be consistent with the representatives s and x, y, z used for the lower levels. Since the KKP approximation gave only fair agreement for the E_0 edge, we have not evaluated the matrix elements for these transitions. But we note that the observation of anisotropies is consistent with the Keldysh approximation and not with the simple theory.

The anisotropies are not simple, but are field dependent, as seen from Fig. 6. The peak-to-peak amplitudes at 115 kV cm^{-1} are in proportion as 0.87, 1.39, and[21] 0.82 for the E_0', $E_0'+\Delta_0'$, and $E_0'+\Delta_0'+\Delta_0$ transitions, for $[1\bar{1}0]$-vs-[001] polarization. The asymmetry of the line shapes also changes, as is seen most clearly with the $E_0'+\Delta_0'$ structure. This structure actually can be decomposed theoretically into four components since it alone of the triplet begins and ends at orbitally degenerate critical points. The four components involve all combinations among the light- and heavy-hole valence band, and the light- and heavy-electron conduction band. It is reasonable to suppose

that the heavy-hole–heavy-electron transition may show a stronger electron-hole interaction ($\sim \mu_{\parallel}^2$ in the two-dimensional Coulomb-continuum threshold) or may even have local M_1 symmetry. According to this interpretation, the heavy components show larger matrix elements for $\hat{e} \parallel [1\bar{1}0]$ by Fig. 6. The shorter period of the Franz-Keldysh oscillations for $\hat{e} \parallel [1\bar{1}0]$ also shows the heavy components are favored for this polarization.

Effective masses have been determined from the Franz-Keldysh oscillations as reported previously[13] and are given in Table I. Interference of light- and heavy-band spectra prevent us from obtaining mass values for $\hat{e} \parallel [1\bar{1}0]$, [001], or $[1\bar{1}0]$ for E_0', $E_0'+\Delta_0'$, or $E_0'+\Delta_0'+\Delta_0$ transitions, respectively. The interference gives further evidence of the importance of matrix-element effects for these transitions.

Critical-point energies and broadening parameters obtained from low-field spectra are given in Table I. The energies are somewhat different from those we obtained earlier,[1] but we believe that the current results are more reliable. The broadening parameters are small, consistent with the Γ-symmetry results that we observed in GaAs.[2]

The line-shape asymmetries of the E_0' triplet are substantially different from their expected values. Table I shows these are of the order of 75°. This appears to be a characteristic of these transitions:

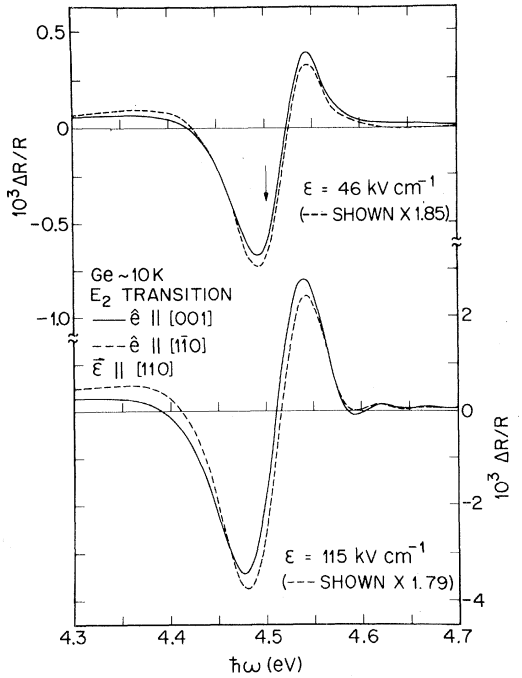

FIG. 7. Representative Schottky barrier ER spectra of the E_2 transition in Ge at 10 K. The field $\vec{\mathcal{E}} \parallel [110]$. The upper and lower pairs are low-field and intermediate-field spectra, respectively. The critical-point energy is indicated by an arrow in the upper curves.

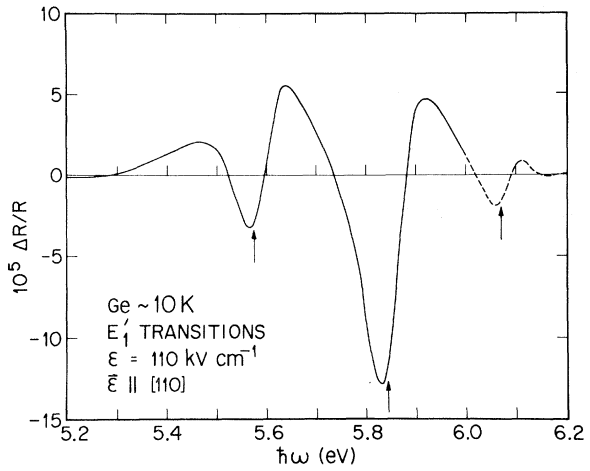

FIG. 8. Representative Schottky barrier ER spectra of the E_1' transition group in Ge at 10 K. Nominally unpolarized light was used to obtain these low-field spectra. Critical point energies are indicated by arrows.

previous depletion-barrier ER measurements in both electrolyte[65] and Schottky-barrier[2] configurations show the same basic line shapes. The discrepancy could be explained by invoking a M_1 model line shape, but this seems to be unrealistic for these transitions. A more likely explanation is that the Coulomb interaction is strong.

D. E_2 transition

The E_2 transition, generally thought to originate from a wide region of the Brillouin zone, was shown to exhibit Franz-Keldysh oscillations.[13] Subsequently, its location was identified by band-structure calculations to be near the $(\frac{3}{4}, \frac{1}{4}, \frac{1}{4})$ points in the Brillouin zone.[66] Representative spectra are shown in Fig. 7. A substantial polarization anisotropy is present, of the order of 1.85 for the low-field results. If $\vec{\mathcal{E}} \parallel [1\bar{1}0]$, the maximum anisotropy that can be obtained with only positive masses is $\frac{3}{2}$ (for 100 critical points). The appearance of such a large anisotropy is therefore proof that at least one negative mass must be involved in the transition. But at least one mass must be positive since the Franz-Keldysh oscillations extend to the high-energy side of the critical-point threshold.

We find further support for a saddle-point interpretation in the line-shape asymmetry. Using Fig. 1 and the usual two-dimensional M_0 model, we calculate a phase deficit $\Delta\theta = 220°$. All but 40° could be removed by assuming an M_2 character, but in view of the phase deficits observed for the E_0' transitions one cannot conclude uniquely that the critical point is M_2 rather than M_1. By comparison of the ER spectra with ellipsometric data,[67] the E_2 structure is seen to occur about half way down the high-energy side of the E_2 peak in ϵ_2. The appear-

ance of a critical-point structure in a spectral region where ϵ_2 is falling with increasing energy is further evidence for a saddle-point character.

The effective mass of the critical point of the E_2 structure has been calculated from the period of the Franz-Keldysh oscillations. The value of the mass is in good agreement with a $\vec{k}\cdot\vec{p}$ two-band-model calculation

$$m_e/\mu^* = 4P^2/mE_g = (0.120)^{-1} ,$$

where $E_g = 4.50$ eV and $P = 2\pi/a_0$, and $a_0 = 10.691a_B$[68] is the lattice constant of Ge. Although the model calculation is greatly oversimplified the agreement is satisfactory.

E. E_1' transitions

The unpolarized-light spectrum for the E_1' transition set in Ge is shown in Fig. 8. These structures are expected to occur at or near [111] symmetry regions in the Brillouin zone.

The critical-point energies and broadening parameters of the three spectral features in the E_1' complex are given in Table I. The amplitude of the third spectral feature at 6070 meV is very small because of the scattered light in our optical system at these energies. Since these data were taken, we have reconfirmed the existence of this feature by synchrotron radiation measurements.[32]

The separation energy between the lower two critical-point energies is 266 ± 10 meV, substantially less than the spin-orbit splitting, $\Delta_1 = 184 \pm 2$ meV, seen for the E_1 and $E_1 + \Delta_1$ structures. Therefore, the transitions giving rise to these structures cannot involve critical points at the same location in the Brillouin zone.[21] Guizzetti *et al.*[31] have also observed this discrepancy in thermoreflectance on a number of semiconductors. A similar discrepancy has been seen in synchrotron radiation ER measurements on GaAs.[33]

The phase deficits for these structures are given in Table I, based on Fig. 1 and the two-dimensional M_0 model. The values are very large, of the same order as the E_2 transition. This suggests that the critical points responsible are possibly also of a saddle-point nature.

[1] D. E. Aspnes, Phys. Rev. Lett. 28, 913 (1972).
[2] D. E. Aspnes and A. A. Studna, Phys. Rev. B 7, 4605 (1973).
[3] For a current review, see Y. Hamakawa and T. Nishino, in *Optical Properties of Solids: New Developments*, edited by B. O. Seraphin (North-Holland, Amsterdam, to be published).
[4] D. E. Aspnes and J. E. Rowe, Solid State Commun. 8, 1145 (1970); Phys. Rev. B 5, 4022 (1972).
[5] D. E. Aspnes, Surf. Sci. 37, 440 (1973).
[6] D. E. Aspnes, Phys. Rev. Lett. 28, 168 (1972).
[7] L. V. Keldysh, Zh. Eksp. Teor. Fiz. 33, 994 (1957) [Sov. Phys.–JETP 6, 763 (1958)]; W. Franz, Z. Naturforsch. A 13, 484 (1958).
[8] D. E. Aspnes, Phys. Rev. 147, 554 (1966); 153, 972 (1967).
[9] Y. Hamakawa, F. A. Germano, and P. Handler, Phys. Rev. 167, 703 (1968).
[10] P. Handler, S. N. Jasperson, and S. Koeppen, Phys. Rev. Lett. 23, 1387 (1969).
[11] P. Handler, S. N. Jasperson, and S. Koeppen, in *Electronic Density of States*, edited by L. H. Bennett, Natl. Bur. Stands. Special Publ. No. 323, (U.S. GPO, Washington, D.C., 1971), p. 417.
[12] T. Nishino and Y. Hamakawa, J. Phys. Soc. Jpn. 26, 403 (1969).
[13] D. E. Aspnes, Phys. Rev. Lett. 31, 230 (1973).
[14] D. E. Aspnes, Phys. Rev. B 10, 4228 (1974).
[15] J. C. Phillips, Phys. Rev. 146, 584 (1966).
[16] B. O. Seraphin, in *Optical Properties of Solids*, edited by E. D. Haidemenakis (Gordon and Breach, New York, 1969), p. 213.
[17] N. Bottka and J. E. Fischer, Phys. Rev. B 3, 2514 (1971).
[18] V. Rehn, Surf. Sci. 37, 443 (1973).
[19] L. V. Keldysh, O. V. Konstantinov, and V. I. Perel', Fiz. Tekh. Poluprovodn. 3, 1042 (1969) [Sov. Phys.–Solid State 3, 876 (1970)].
[20] R. Enderlein, in *Proceedings of the Twelfth International Conference on the Physics of Semiconductors*, edited by M. Pilkuhn (Teubner, Stuttgart, 1974), p. 161.
[21] D. E. Aspnes and A. A. Studna, Bull. Am. Phys. Soc. 18, 438 (1973).
[22] J. E. Rowe and D. E. Aspnes, Phys. Rev. Lett. 25, 162 (1970).
[23] D. E. Aspnes, J. Opt. Soc. Am. 63, 1380 (1973). The linear expansion [Eq. (2.11)] in this reference is correct; the equivalent, Eq. (3.2), in Ref. 2 is missing a factor n which should multiply the first-order correction term.
[24] D. E. Aspnes and A. Frova, Phys. Rev. B 2, 1037 (1970); B 3, 1511 (1971).
[25] D. E. Aspnes, P. Handler, and D. F. Blossey, Phys. Rev. 166, 921 (1968).
[26] H. D. Rees, J. Phys. Chem. Solids 29, 143 (1968).
[27] P. Lawaetz, Phys. Rev. B 4, 3460 (1971).
[28] D. E. Aspnes and J. E. Rowe, in *Proceedings of the Tenth International Conference on the Physics of Semiconductors*, edited by S. P. Keller, J. C. Hensel, and F. Stern, Publication No. CONF-70080/U.S. AEC, Oak Ridge, Tenn., 1970), p. 422.
[29] T. M. Donovan, J. E. Fischer, J. Matsuzaki, and W. E. Spicer, Phys. Rev. B 3, 4292 (1971).
[30] K. C. Pandy and J. C. Phillips, Phys. Rev. B 9, 1560 (1974).
[31] G. Guizzetti, L. Nosenzo, E. Reguzzoni, and G. Samoggia, Phys. Rev. B 9, 640 (1974).
[32] D. E. Aspnes and C. G. Olson (unpublished).
[33] D. E. Aspnes, C. G. Olson, and D. W. Lynch, Phys. Rev. B 12, 2574 (1975).
[34] D. E. Aspnes and A. Frova, Solid State Commun. 7, 155 (1969).
[35] A. A. Studna, Rev. Sci. Instrum. 46, 735 (1975).
[36] D. E. Aspnes and J. E. Fischer, Comments Solid State Phys. 4, 159 (1972).
[37] D. E. Aspnes, in *Proceedings of the Eleventh Inter-*

national Conference on the Physics of Semiconductors edited by M. Miasek (PWN, Warszawa, 1972), p. 1371.
[38]J. E. Fischer and N. Bottka, Phys. Rev. Lett. 24, 1292 (1970).
[39]E. J. Johnson, in *Semiconductors and Semimetals*, edited by R. K. Willardson and A. C. Beer (Academic, New York, 1967), Vol. 3, p. 153.
[40]R. Enderlein, R. Keiper, and W. Tausenfreund, Phys. Status Solidi 33, 69 (1969).
[41]E. O. Kane, J. Phys. Chem. Solids 1, 82 (1956).
[42]L. I. Schiff, *Quantum Mechanics* (McGraw-Hill, New York, 1955), p. 156.
[43]G. G. Macfarlane, T. P. McLean, J. E. Quarrington, and V. Roberts, Proc. Phys. Soc. Lond. 71, 863 (1958).
[44]J. M. Luttinger, Phys. Rev. 102, 1030 (1956).
[45]S. Koeppen and P. Handler, Phys. Rev. 187, 1182 (1969).
[46]D. E. Aspnes and J. E. Rowe, Phys. Rev. Lett. 27, 188 (1971).
[47]D. F. Blossey, Phys. Rev. B 2, 3976 (1970); B 3, 1382 (1971).
[48]F. C. Weinstein, J. D. Dow, and B. Y. Lao, Phys. Rev. B 4, 3502 (1971).
[49]R. J. Elliott, Phys. Rev. 108, 1384 (1957)
[50]V. A. Tyagai, V. N. Bondarenko, and O. V. Snitko, Fiz. Tekh. Poluprovodn. 5, 1038 (1971) [Sov. Phys.–Semicond. 5, 920 (1971)].
[51]F. Evangelisti, A. Frova, and J. U. Fischbach, Phys. Rev. Lett. 29, 1001 (1972); Surf. Sci. 37, 841 (1973).
[52]T. Nishino, T. Yanagida, and Y. Hamakawa, J. Phys. Soc. Jpn. 30, 579 (1971).
[53]The value given in Ref. 12 for E_{ex} is 872 meV, calculated from the negative extremum of their line shapes. The value, 879 meV, given in the text, is obtained from their 9-kV cm^{-1} spectrum using the three-point method.
[54]G. Bordure, C. Alibert, and M. Averous, in *Proceedings of the Eleventh International Conference on the Physics of Semiconductors*, edited by M. Miasek (PWN, Warszawa, 1972), p. 1426.
[55]D. D. Sell, S. E. Stokowksi, R. Dingle, and J. V. DiLorenzo, Phys. Rev. B 7, 4568 (1973).
[56]J. E. Fischer, in *Proceedings of the Tenth International Conference on the Physics of Semiconductors*, edited by S. P. Keller, J. C. Hensel, and F. Stern, publication No. CONF-700801 (U.S. AEC, Oak Ridge, Tenn., 1970), p. 427.
[57]These values are slightly different than the average values calculated in Ref. 27.
[58]The density-of-states prefactor fot the Coulomb continuum step edge is proportional to μ^2 [see, e.g., Eq. (4.7) of Ref. 24] and that of a three-dimensional critical point is proportional to $\mu^{3/2}$. These must be reduced by the mass dependence of the prefactor $(\hbar\Omega)^n$. For intermediate fields, $n=0$ and $\frac{1}{2}$, respectively, for two- and three-dimensional edges. At low fields, $n=3$. The data probably correspond to some intermediate value of n. We used the intermediate-field three-dimensional value in the text.
[59]R. A. Forman, D. E. Aspnes, and M. Cardona, J. Phys. Chem. Solids 31, 227 (1970).
[60]J. Grover, S. Koeppen, and P. Handler, Phys. Rev. B 4, 2830 (1971).
[61]D. D. Sell and E. O. Kane, Phys. Rev. 185, 1103 (1969).
[62]G. Dresselhaus and M. S. Dresselhaus, Phys. Rev. 160, 649 (1967).
[63]K. C. Pandey and J. C. Phillips, Phys. Rev. B 9, 1560 (1974).
[64]S. O. Sari, Solid State Commun. 12, 705 (1973); Phys. Rev. Lett. 30, 1323 (1973); Phys. Rev. B 10, 599 (1974).
[63]D. E. Aspnes (unpublished).
[66]J. R. Chelikowski and M. L. Cohen, Phys. Rev. Lett. 31, 1582 (1973).
[67]D. E. Aspnes, in *Proceedings of the Twelfth International Conference on the Physics of Semiconductors*, edited by M. Pilkuhn (Teubner, Stuttgart, 1974), p. 1197.
[68]J. A. Van Vechten, Phys. Rev. 182, 891 (1969).